

Microwave Measurements with Lake Shore Probe Stations

1. INTRODUCTION

This application note explores using the Lake Shore Cryotronics Model TTP4 probe station to make microwave measurements using ground-signal-ground (GSG) microwave probes. While larger Lake Shore probe stations have slightly more loss due to the longer arm lengths, the frequency responses of the larger systems are similar to the ones presented here. The probe station/probe performance over the operating frequency range is assessed using the Anritsu 37397D vector network analyzer (VNA), which has measurement capability from 40 MHz to 65 GHz. The highest frequency probe that we sell with the probe stations is 67 GHz, so for all practical purposes we can make measurements over the whole probe station bandwidth. Measurement results showing the frequency response are presented, as well as measurements showing the necessity of planarization and the benefits of calibration. Measurement results were taken at room temperature and cryogenic temperatures.

2. TTP4 PROBE STATION

The TTP4 is a versatile cryogenic micro-manipulated probe station used for non-destructive testing of devices on full and partial wafers up to 51 mm (2 in) in diameter. The TTP4 is a platform for measurement of electrical, electro-optical, parametric, high Z, DC, RF, and microwave properties of materials and test devices. Nanoscale electronics, quantum wires and dots, and semiconductors are typical materials measured in a TTP4. A wide selection of probes, cables, sample holders, and options makes it possible to configure the TTP4 to meet your specific measurement applications.

The TTP4 operates over a temperature range of 4.2 K to 475 K. With options, the base temperature can be extended down to 3.2 K. The probe station provides efficient temperature operation and control with a continuous refrigeration system using either helium or nitrogen. Vapor-cooled shielding optimizes efficiency and intercepts blackbody radiation before it reaches the sample. Two control heaters on the cold head minimize temperature gradients across the sample and, along with the radiation shield heater, provide the probe station with fast thermal response.

The TTP4 includes up to four ultra-stable micro-manipulated stages, which give the user precise 3-axis control of the probe position to accurately land the probe tip on the device features. Proprietary probe tips in a variety of sizes and materials minimize thermal mass and optimize electrical contacts to the device under test (DUT). Probe tips are thermally linked to the cold head to minimize heat transfer to the DUT.

For increased versatility, TTP4 options include a 3.2 K base temperature stage, vibration isolation systems, LN₂ Dewar kit, higher magnification monoscopes, vacuum turbo pumping system, supplemental radiation shield temperature control, and probe arm fiber optic cable.



3. MICROWAVE PROBES

The microwave probes that we use with our systems are GGB PicoProbe® Ground-Signal-Ground (GSG) style, which means that the probe tip consists of a signal tip in the middle with a ground tip on either side of it. You may hear these probes referred to as “PicoProbe”, “GGB”, or “GSG” probe — all refer to the same probe type. The three different frequencies of probes each have a different connector type, and except for the model/serial number, the connector is the only way to differentiate between the probes. The table below details the three probe frequency ranges and associated connectors, as well as to which connectors they can mate.

Highest rated frequency	Connector	Mates with
40 GHz	K-type (2.92 mm)	Standard SMA connectors
50 GHz	2.4 mm	V (1.85 mm) connectors
67 GHz	V-type (1.85 mm)	2.4 mm connectors

For reference, Figures 1-3 show male, female, and head-on views of the three types of connectors. **Note that all three connector types look very similar!** Side by side, differences in the connectors can be seen primarily in the head-on view in the thickness of outer conductor and spacing between the inner and outer conductor. Care must be taken to ensure that the correct cable/connection is made when using various probes.



FIGURE 1: K-type (2.92 mm) connectors — published mode free to 40 GHz



FIGURE 2: 2.4 mm connectors — published mode free to 50 GHz



FIGURE 3: V-type (1.85 mm) connectors — published mode free to ~65 GHz

The spacing between the GSG tips of the microwave probes is referred to as the probe pitch. The probe pitch is generally measured in micrometers (μm). Probe pitch spacing usually ranges from 50 – 250 μm , although larger and smaller spacing is possible. In general, the smaller the pitch, the better the insertion loss (S_{21}/S_{12}) of a probe; however, when you compare probes of different pitches in the 50 – 250 μm pitch range, the insertion loss difference is minor. The return loss (S_{11}/S_{22}) would be the same for the various pitches as well.

4. MEASUREMENT SCOPE AND SETUP

The Anritsu 37397D Lightning VNA used in these measurements is pictured in Figure 4, with the TTP4 measurement setup shown in Figure 5. The Anritsu VNA has a frequency range of 40 MHz to 65 GHz.



FIGURE 4: Anritsu 37397D Lightning VNA

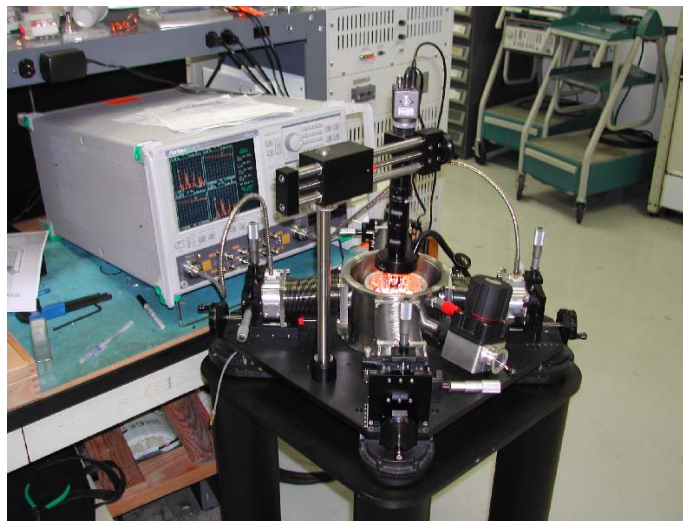


FIGURE 5: TTP4 Probe Station Microwave Measurement Setup with Anritsu 37397D Lightning VNA

Initially, we can calibrate the VNA and its test cables to account for its own frequency-dependent losses such that the virtual measurement reference plane is moved from inside the VNA out to the ends of the VNA test cables. We do this by measuring a series of known test loads; a common calibration is known as a SOLT calibration and involves using a **S**hort, **O**pen, **50 Ω** impedance **L**oad, and **50 Ω** **T**hrough impedance transmission line. After calibrating, we can take a measurement that assesses the overall frequency-dependent [S] parameters of the probe station as a system, without the impact of the VNA and VNA test cables. See section 5.1 for more details.

Taking this one step further, if we want to make a measurement on an unknown device under test (DUT) and exclude the response of both the VNA test cables and the probe station, we can use the GGB CS-5 calibration substrate to 'calibrate out' the probe station losses. We can do this by again doing a SOLT calibration this time using the short, open, 50 Ω load, and 50 Ω through test points on the CS-5 substrate. This moves the virtual measurement reference plane out to the end of the probe tips and should allow us to measure the DUT independent of the VNA test cables and the probe station. The CS-5 calibration substrate and a 40 GHz GSG probe are shown below in Figure 6. See section 5.6 for more details.

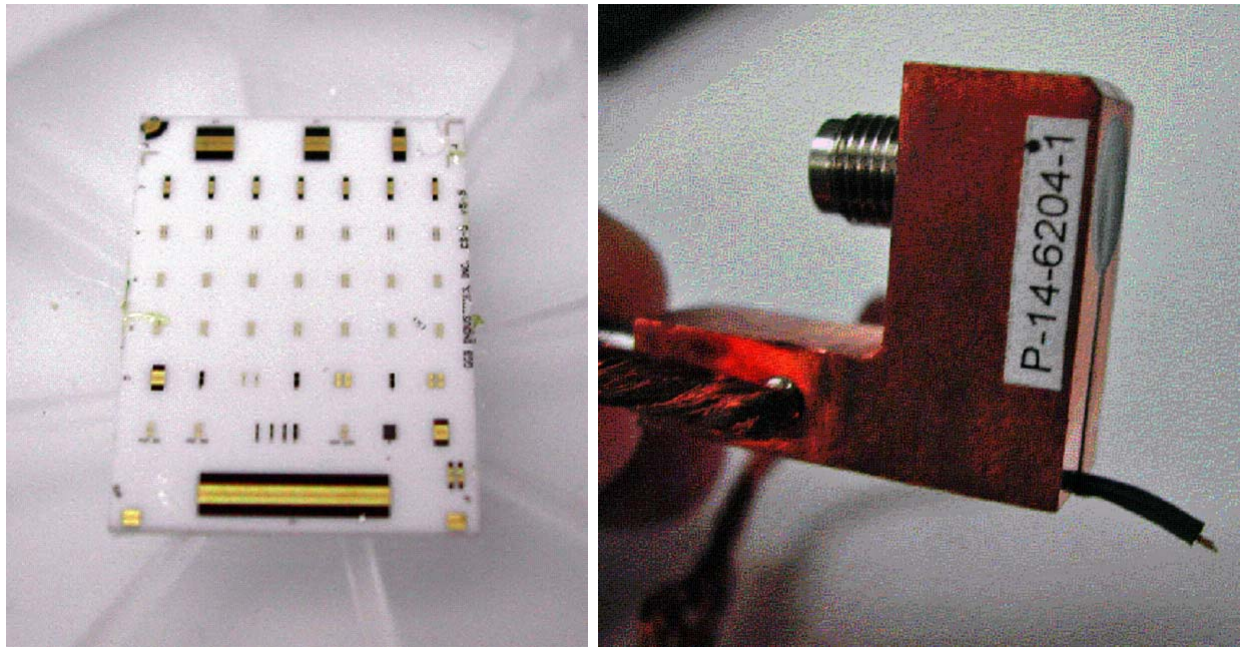


FIGURE 6: CS-5 calibration substrate and GSG 40 GHz probe

The following measurements will be described in the next sections:

- Initial calibration of the Anritsu 37397D VNA (reference plane at end of test cables)
- Frequency response before and after planarization
- 67 GHz probe measurements
- 50 GHz probe measurements
- 40 GHz probe measurements
- Calibration with CS-5 substrate (reference plane at end of probe tips)
- Probe station losses temperature dependence
- Time domain reflectometry (TDR) measurements
- Measurements with a broken probe tip

5. MEASUREMENT RESULTS

The following sections show the frequency response of the TTP4 probe station in various GSG microwave probe scenarios. Unless otherwise noted, the measurements were taken at room temperature.

5.1 Initial Calibration of the Anritsu 37397D VNA

The initial plots in Figure 7 show the frequency response of the Anritsu VNA following full 2-port SOLT calibration using the 1.85 mm connected calibration standard set to place the measurement reference plane at the end of the VNA cables. This means that the losses internal to the VNA and the losses of the VNA cables themselves are calibrated out. The plots in Figure 7 show the response of a 1.85 mm female-female 50 Ω through connecting the two VNA cables together after calibration. This simple measurement gives us a good impedance-matched, low-loss DUT to check the quality of the calibration. (Note that the y axes of these plots are on a dB scale.) The top plot shows the four parameters of the S matrix. Recall that S_{11} and S_{22} represent the reflection coefficients of ports 1 and 2, respectively. S_{21} and S_{12} represent the transmission coefficients of port 1 to 2 and port 2 to 1, respectively. See Appendix A for a discussion of S parameters.

Since the DUT is a through that is matched to the 50 Ω impedance of the test ports, ideally the transmission coefficients should be unity (0 dB) and the reflection coefficients should be zero ($-\infty$ dB). What we are looking for in a real measurement for this DUT is S_{21}/S_{12} to follow along the 0 dB line as close as possible and for S_{11}/S_{22} to be as low as possible across the frequency range. The bottom plot shows a magnified view of the transmission coefficients S_{21} and S_{12} . Evaluating both plots in Figure 7, we can see that we do in fact have a good calibration of the Anritsu VNA. Figure 7 can be used as a best-case reference to compare to the remainder of the measurements in this application note.

We can now use the calibrated VNA to assess the frequency-dependent losses with the probe station as our DUT across the 40 MHz to 65 GHz band. These system-level measurements will take into account any factors that would impede a microwave measurement, so in the measurements of the remaining sections great care was taken to make sure that connectors were tightened to the proper torque, GSG probes properly planarized, and the probe tips well seated on the measurement pads.

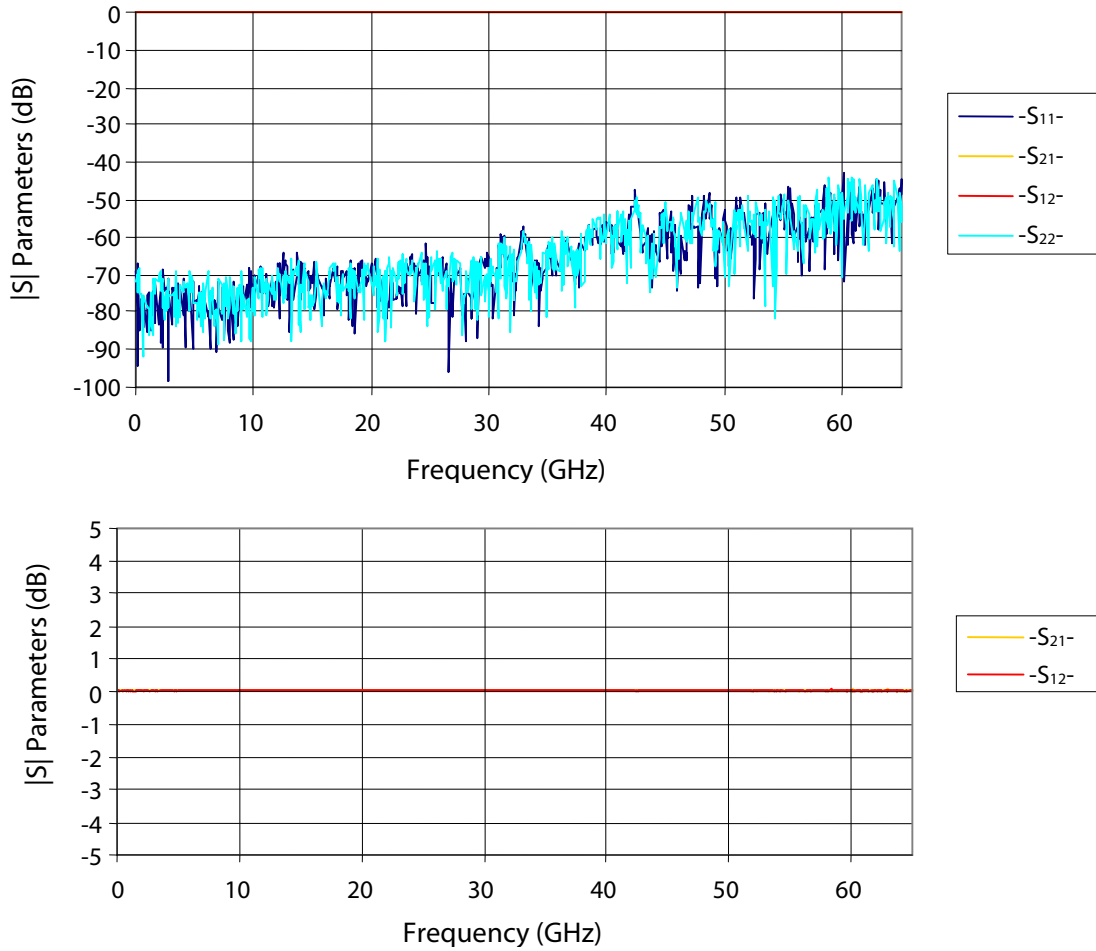


FIGURE 7: SMA connected 50 Ω through following Anritsu VNA full 2-port calibration to place reference planes at end of VNA flexible test cables

5.2 Frequency Response Before and After Planarization

Since the GSG probes have three probe tips that all have to land on individual pads, aligning the probe so that the tips are planar (i.e., all tips land with good contact) is very important to ensure reliable measurements. Figures 8 and 9 show the S parameters of a pair of microwave probes on a through test point before and after planarization. In comparing the two figures, the importance of planarization is clear in the improvement in both the transmission and reflection coefficients of Figure 9.

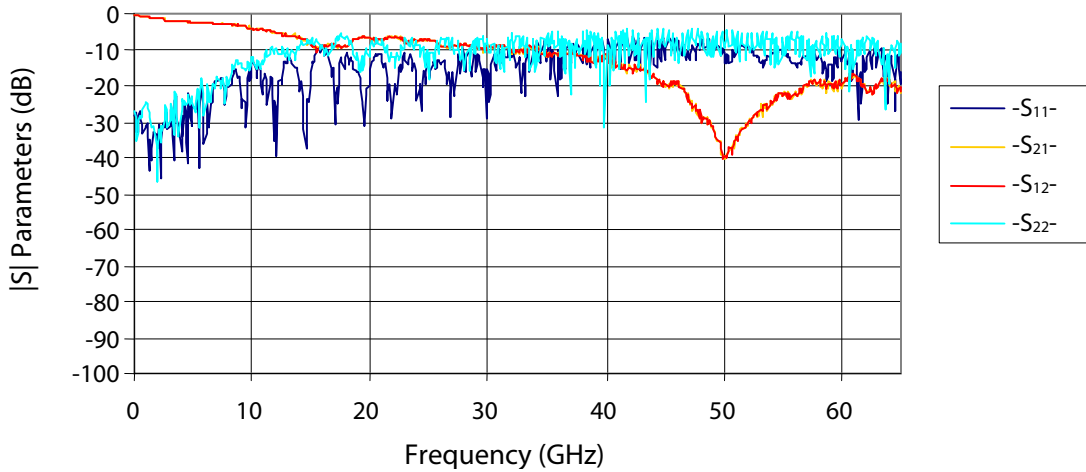


FIGURE 8: GSG probes prior to proper planarization

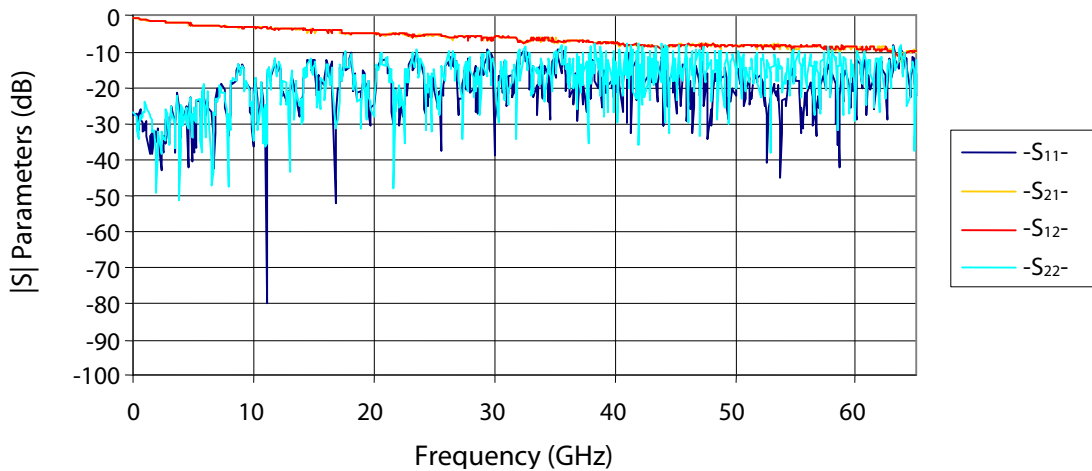


FIGURE 9: GSG probes after proper planarization

5.3 67 GHz Probe Measurements

Figure 10 shows the response of a pair of 150 μm pitch 67 GHz probes from 40 MHz to 65 GHz placed on a 50 Ω through test structure on the CS-5 calibration substrate. The measurements were made using the calibration described in Section 4.1 that places the measurement reference plane at the 1.85 mm input connectors of the 67 GHz probe arms. Thus, the figures below show the frequency-dependent characteristics of the TTP4 probe station with the 67 GHz probes and probe arms. Note that for comparison the plots in Figure 10 are on the same scale as Figure 7. The transmission coefficients S_{21}/S_{12} remain above -10 dB and the reflection coefficients S_{11}/S_{22} remain below -10 dB over the entire frequency band. The gradual sloping increase in loss (i.e., decrease in S_{21}/S_{12}) as the frequency increases is expected. Considering the number of places in the signal path susceptible to reflection (see Section 5.8), the overall S_{11}/S_{22} reflection performance is good. (The 65 GHz data below is easily extrapolated to 67 GHz, as there is no physical system mechanism that would cause a sharp drop in performance in the last 2 GHz.)

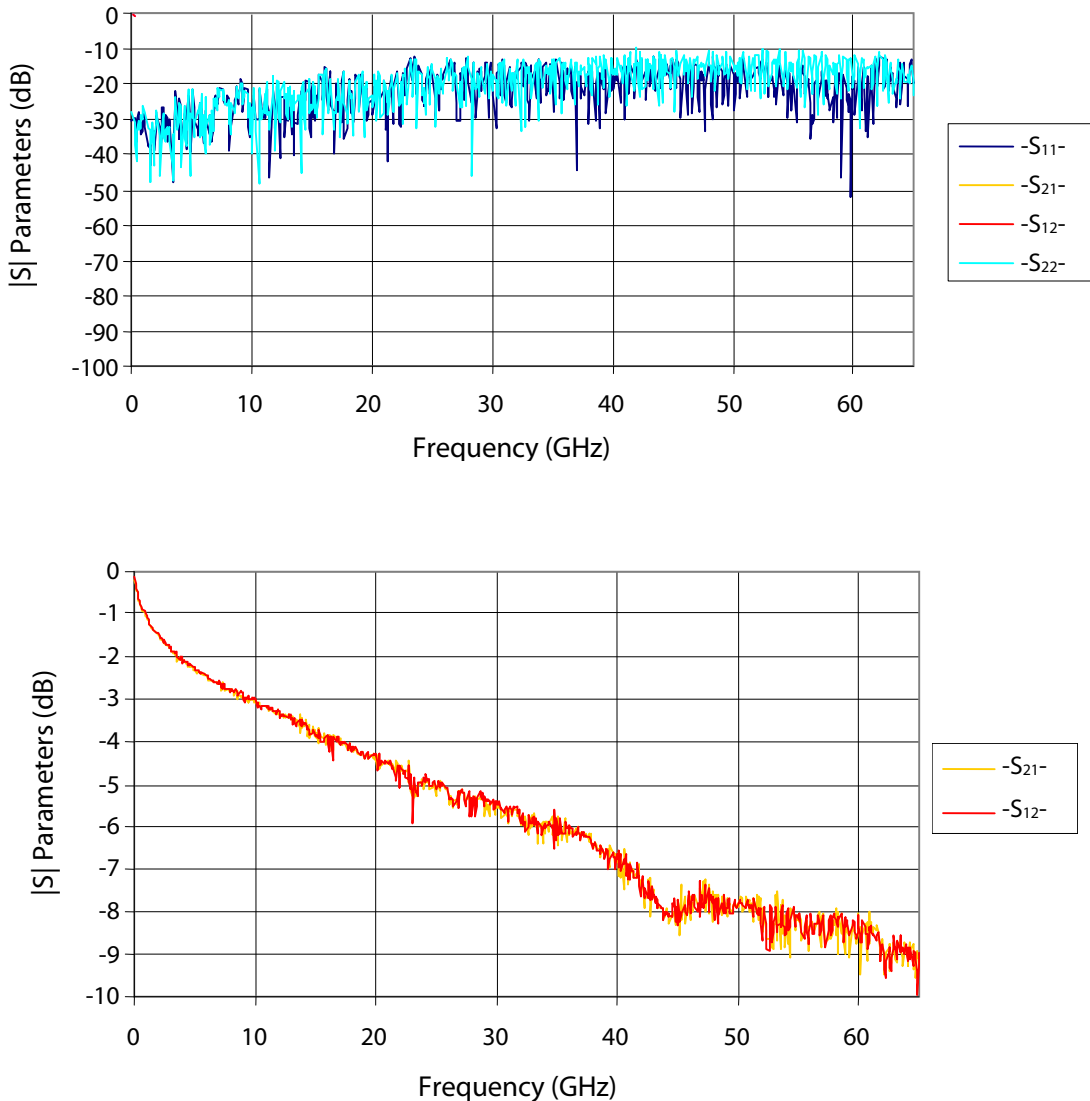


FIGURE 10: Through measurement with properly planarized 67 GHz GSG probes

5.4 50 GHz Probe Measurements

Figure 11 shows the response for a pair of 200 μm pitch 50 GHz probes placed on a 50 Ω through test structure on the CS-5 calibration substrate. The measurements were made using the calibration that places the measurement reference plane at the 2.4 mm input connectors of the 50 GHz probe arms. Thus, the figures below show the frequency-dependent characteristics of the TTP4 probe station with the 50 GHz probes and associated probe arms. Note that the plots in Figure 10 are on the same scale as Figure 7 for comparison. The transmission coefficients S_{21}/S_{12} remain above -10 dB and the reflection coefficients S_{11}/S_{22} remain at or below -10 dB over the entire frequency band. The gradual sloping increase in loss (i.e., decrease in S_{21}/S_{12}) as the frequency increases is expected. The overall S_{11}/S_{22} reflection performance is good.

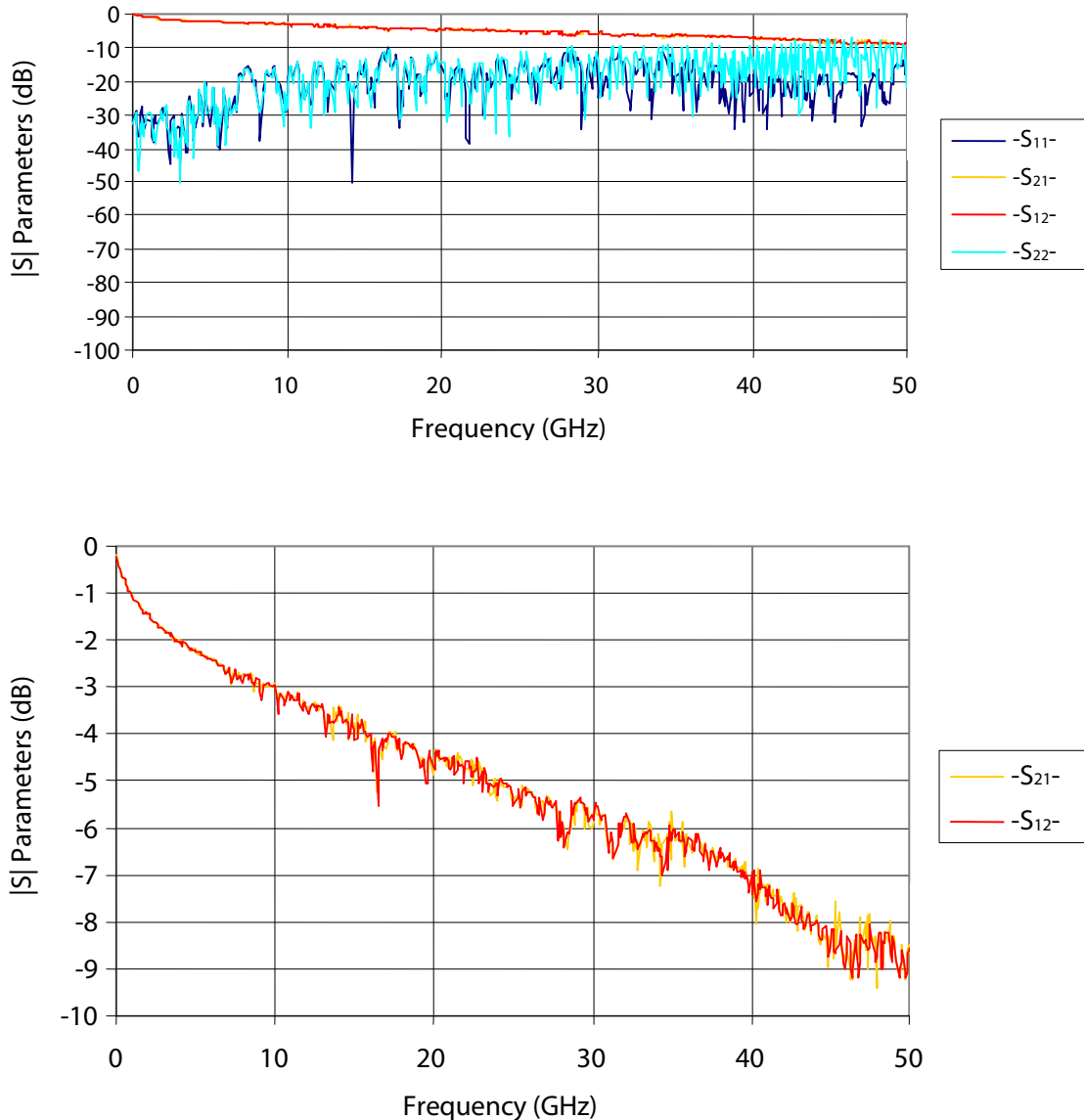


FIGURE 11: Through measurement with properly planarized 50 GHz GSG probes

5.5 40 GHz Probe Measurements

Figure 12 shows the response for a pair of 200 μm pitch 40 GHz probes placed on a 50 Ω through test structure on the CS-5 calibration substrate. The measurements were made using the calibration that places the measurement reference plane at the K-type (2.92 mm) input connectors of the 40 GHz probe arms¹. Thus, the figures below show the frequency-dependent characteristics of the TTP4 probe station with the 40 GHz probes and probe arms. The transmission coefficients S_{21}/S_{12} remain above -10 dB and the reflection coefficients S_{11}/S_{22} remain at or below -10 dB over the entire frequency band. The gradual sloping increase in loss (i.e., decrease in S_{21}/S_{12}) as the frequency increases is expected. The overall S_{11}/S_{22} reflection performance is good.

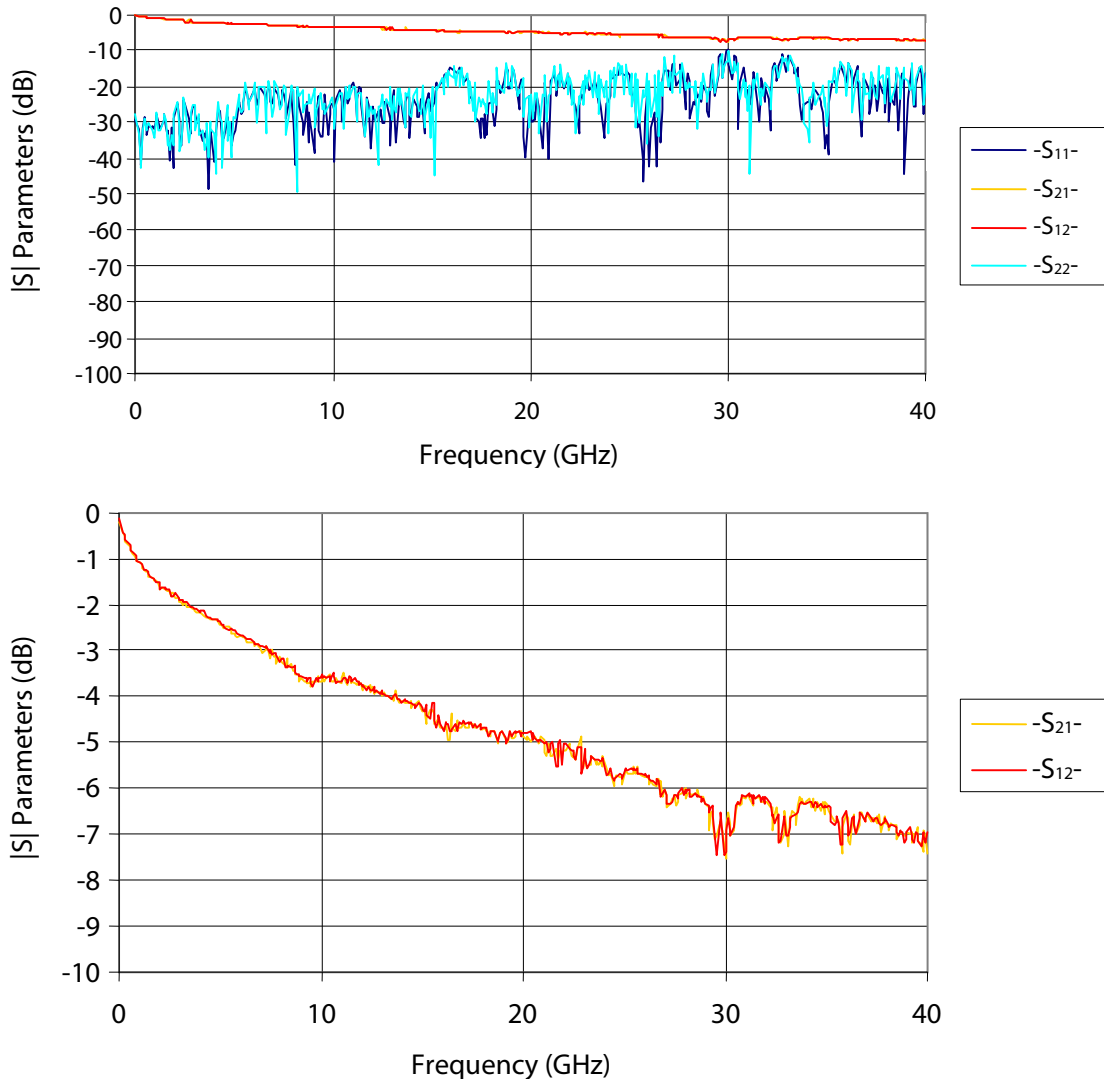


FIGURE 12: Through measurement with properly planarized 40 GHz GSG probes

¹ A K-type to 1.85 mm adapter was placed on both K connector inputs to the probe arms in order to adapt to the 1.85 mm connectors on the VNA cables. The extra two adapters could be some of the cause for reflection ripple in the 40 GHz measurement data, as they could not be calibrated out of the measurement.

5.6 Calibration with CS-5 Substrate

Using the procedure contained in the GGB CS-5 calibration substrate manual, we can do a SOLT calibration to calibrate out the frequency-dependent losses of the probe station and move the measurement reference plane out to the probe tips. Figure 13 shows the results of this calibration on a pair of the 67 GHz microwave probes. Comparing Figure 13 to Figure 10, for example, you can see that we have removed the loss in the transmission coefficients S_{21}/S_{12} and pushed the reflection coefficients S_{11}/S_{22} further down. We can now make a measurement on an unknown DUT and assess its frequency-dependent parameters independently of the probe station's frequency-dependent losses. The SOLT calibration procedure laid out in the CS-5 manual involves placing a pair of probes on four different standard test points for a total of eight probe landing placements. Numerous calibrations were performed with results similar to that found in Figure 13, although ± 0.5 dB at the upper end of the frequency range was not uncommon. It was determined that if in any of the steps of the procedure a probe was not well seated on its pad, variability results. Thus, proper probe landing is extremely important to achieving a good calibration.

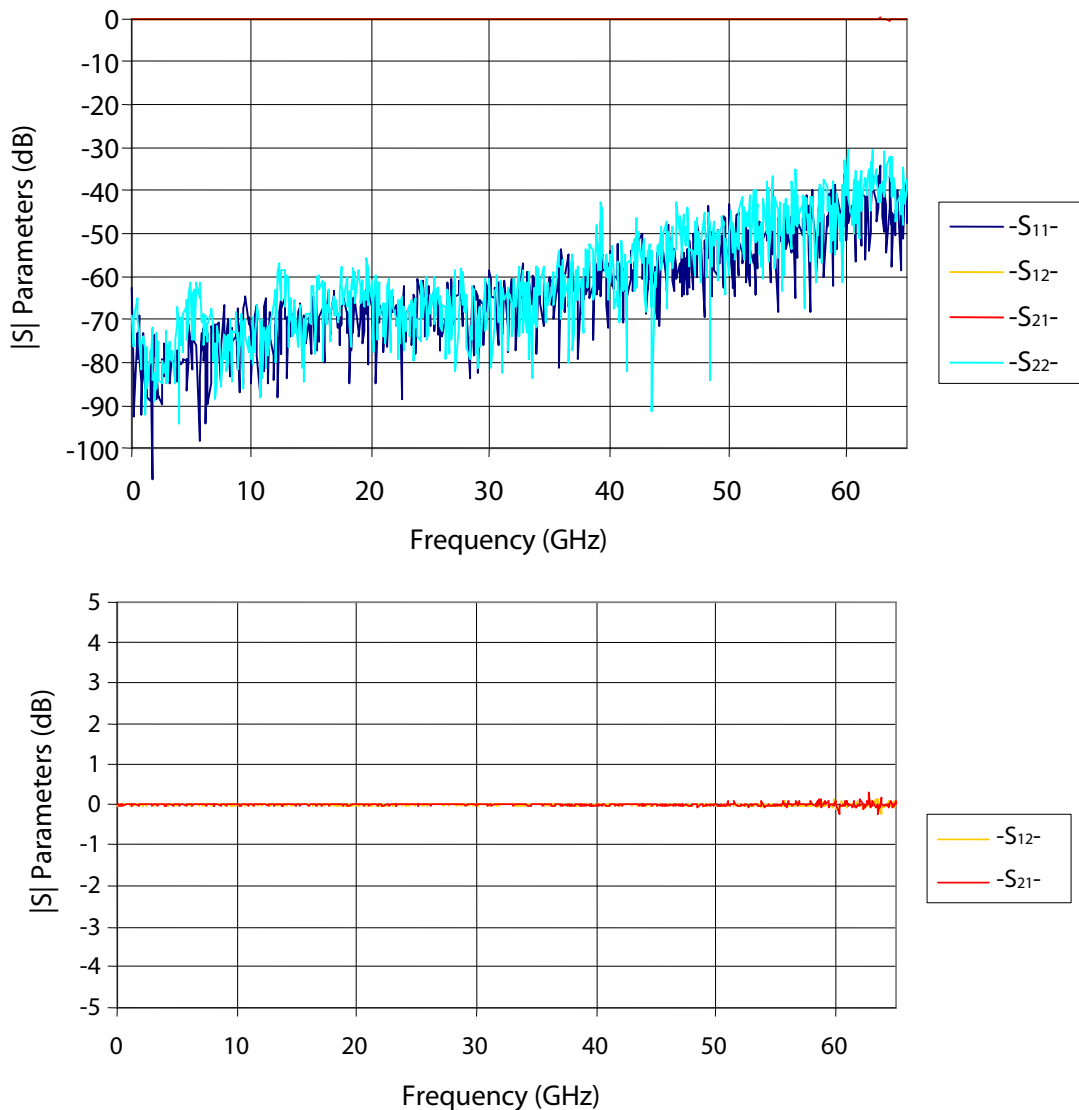


FIGURE 13: Microwave probes after calibration with CS-5 substrate to remove probe station/probe tip losses (Note 10 dB full scale of second plot)

In addition to the procedure for making the calibration, some investigation into the long-term stability of the calibration was done. The calibration shown in Figure 13 was left on the through standard for three hours with no noticeable variation in performance. Both probes were then raised vertically and then lowered back onto the same through pads. The resulting performance is shown in Figure 14. As can be seen, the performance is still very acceptable, however, there is noticeable (albeit small) ripple in the S_{21}/S_{12} and the S_{11}/S_{22} reflection coefficients have risen. With the only difference being the probe placement, this shows the sensitivity of the calibration to probe placement. See Section 5.8 for temperature dependence of calibration.

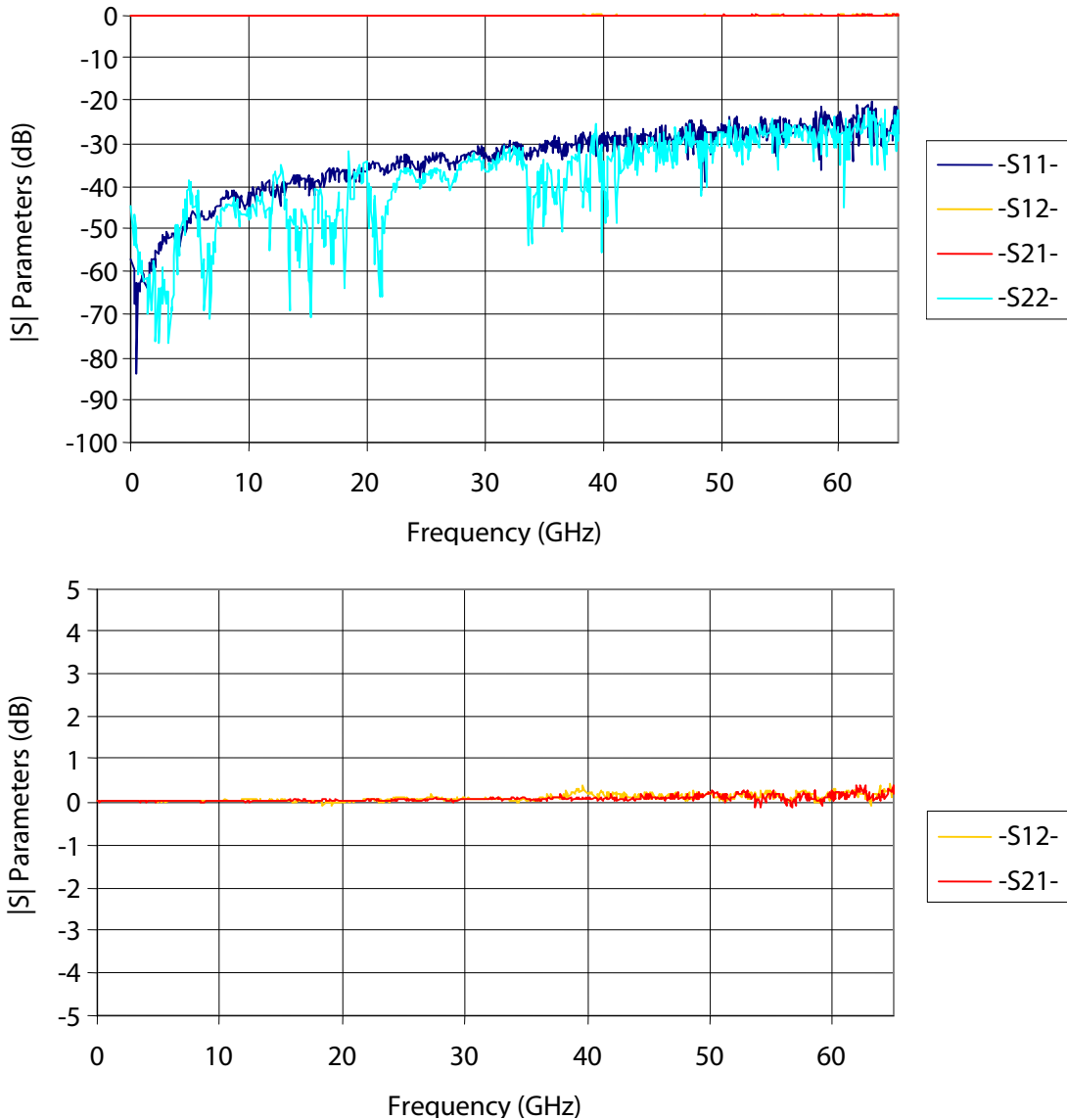


FIGURE 14: Same measurement as in Figure 13, three hours after performing the calibration and after picking up the probes and setting them back down on same through

5.7 Probe Station Losses Temperature Dependence

The following plots show the temperature dependence of the TTP4 probe station frequency response with 67 GHz GSG probes landed on a 50 Ω through of the CS-5 calibration substrate at 300 K, 77 K, and 4.3 K, respectively. Measurements were made with an Anritsu 37397D Lightning VNA, calibrated to place the reference plane at the end of the measurement cables (i.e., with a standard cal kit and prior to using the CS-5 to calibrate out the probe station system losses). As can be seen from the S parameters measured at the various temperatures, there is not a significant temperature dependence on the losses in the system. Note that the probes were raised between measurements to ensure the probe tips were not damaged due to thermal contraction of the probe arms over such large temperature gradients.

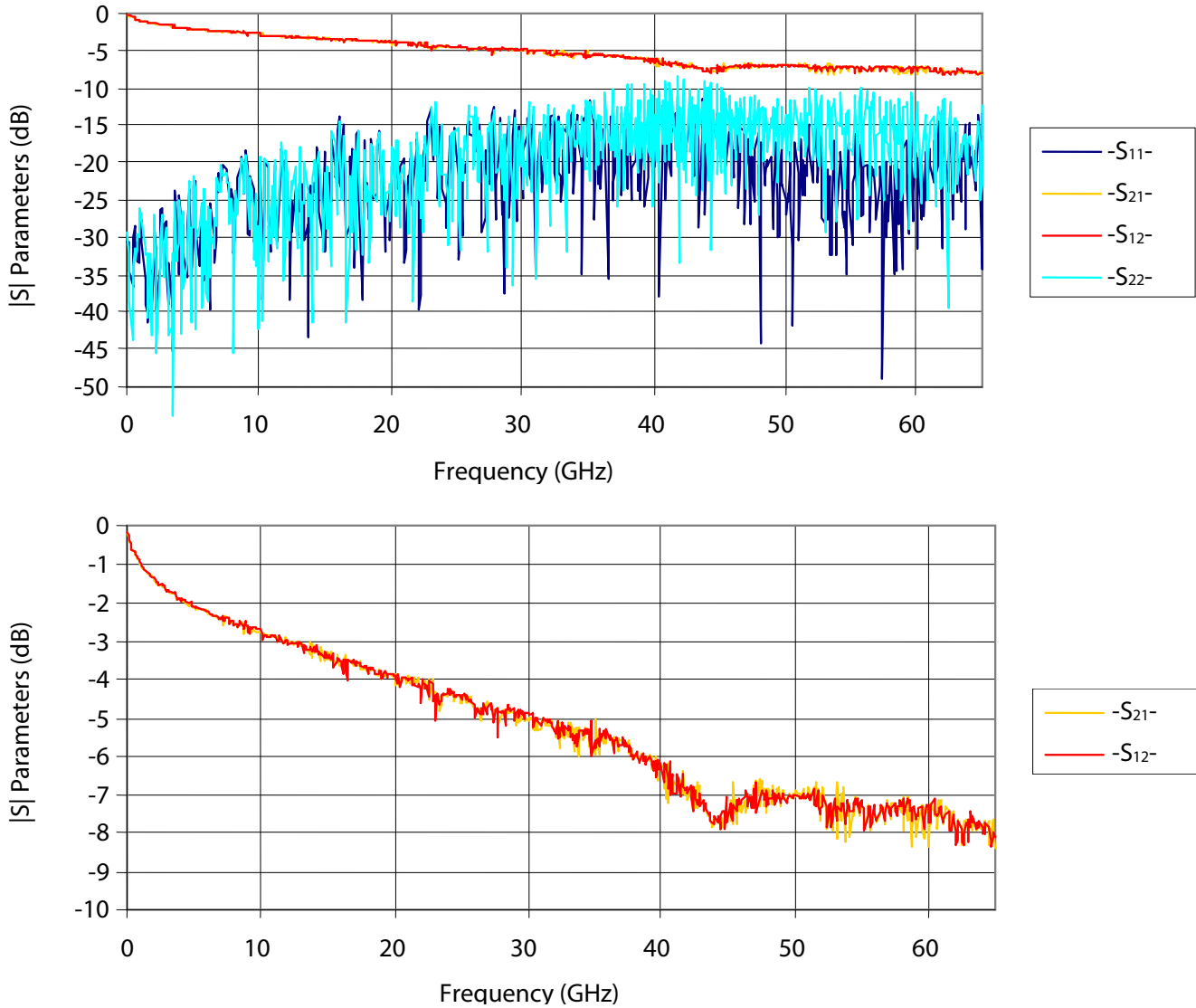


FIGURE 15: Frequency Response at 300 K

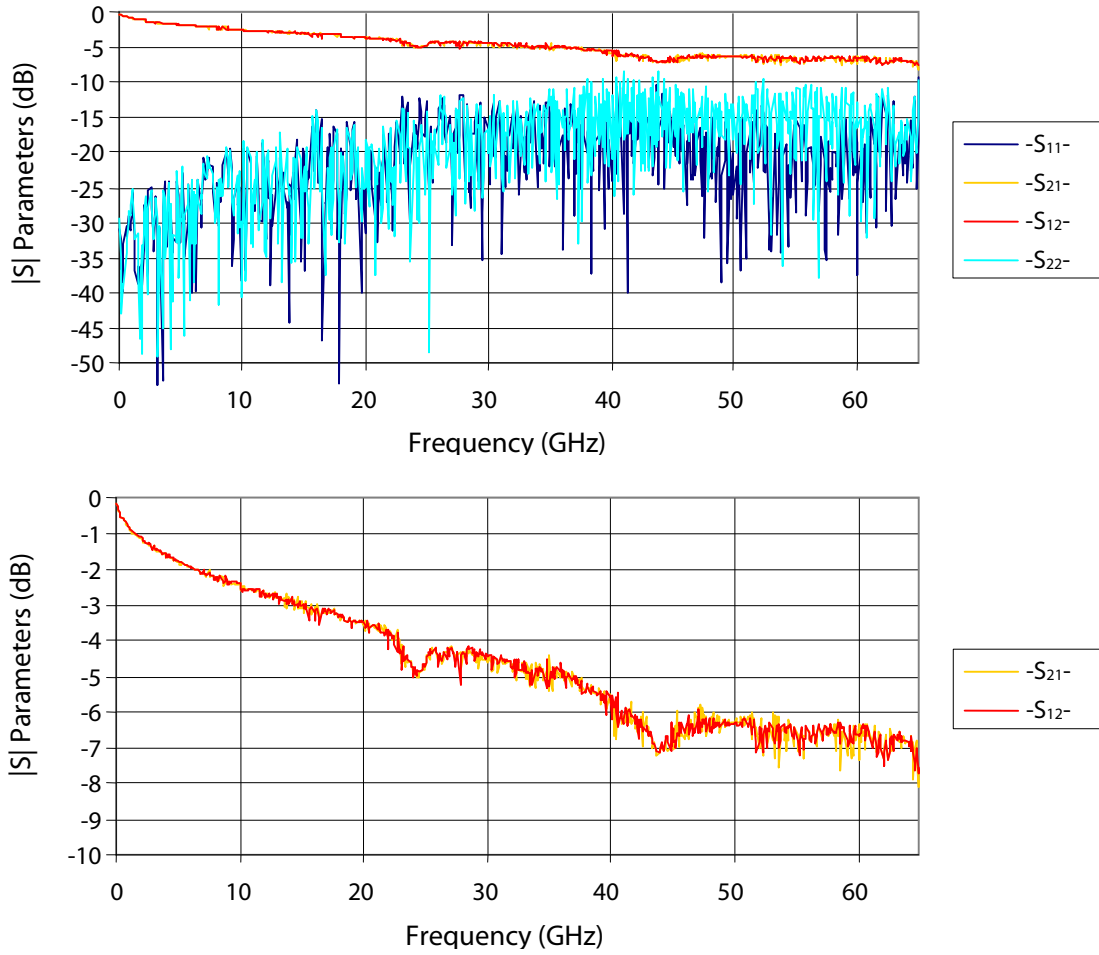


FIGURE 16: Frequency Response at 77 K

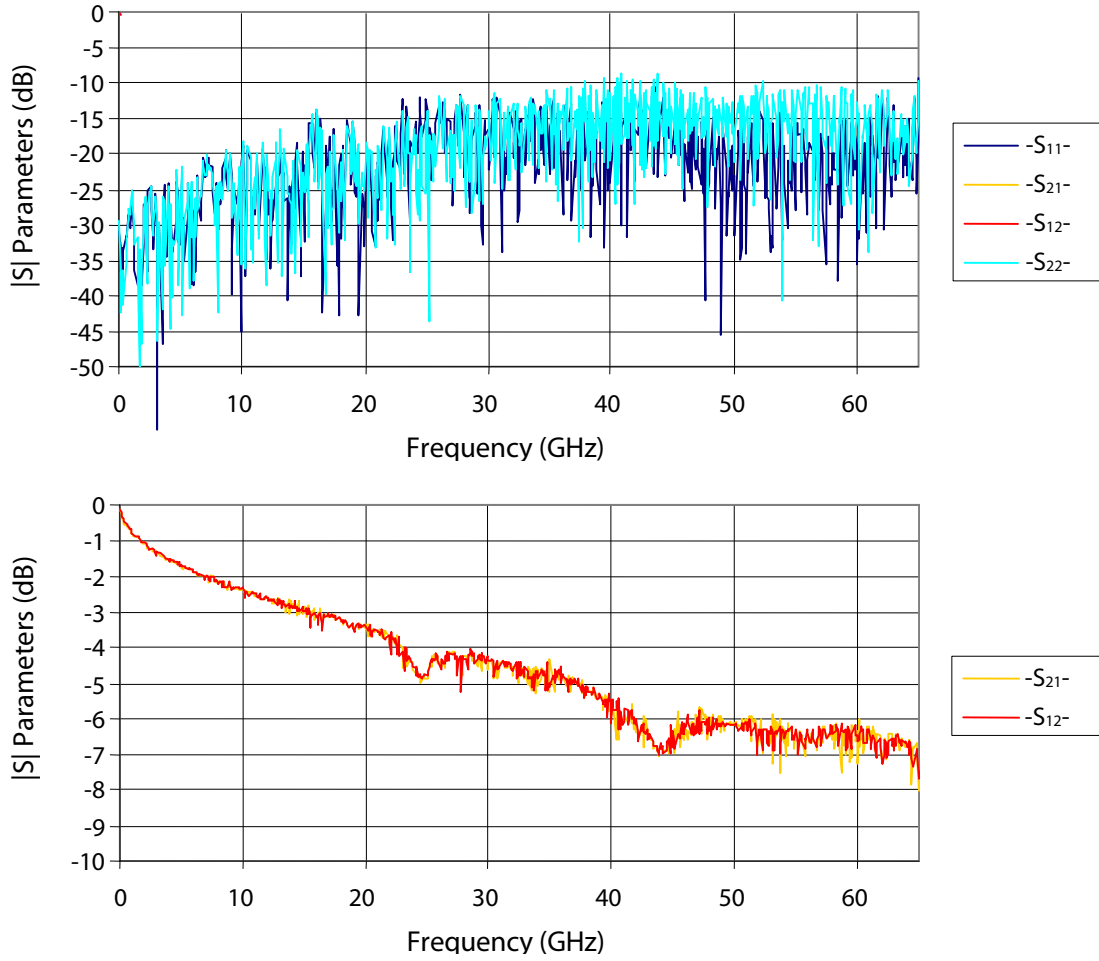


FIGURE 17: Frequency Response at 4.3 K

5.8 Calibration with CS-5 Substrate Temperature Dependence

In making measurements with a VNA at room temperature conditions, it is well understood that thermal variation of the VNA itself or of the test cables and DUT can cause measurement variability when using a standard VNA calibration. Thus, for standard microwave measurements, calibrations are often repeated prior to taking sensitive measurements to ensure accurate results. These same practices should be applied to measurements with the cryogenic probe station. In addition, the large delta in temperatures when transitioning the system from room (~300 K) down to cryogenic temperatures (4 – 77 K) adds additional conditions that must be accounted for when making measurements. A large temperature delta will cause mechanical and electrical changes in the microwave measurement system (i.e., cables, probes, and DUT). Once the components reach a stable thermal equilibrium at a given temperature, however, the electrical microwave measurements will be stable as well. Due to the mechanical changes of the test setup with changing temperature, a calibration performed at room temperature will have some performance variation when that calibration is applied to a measurement at cryogenic temperatures. Figure 18 below shows the measurement of a pair of microwave probes on a through substrate at 4.2 K temperature with a CS-5 calibration performed at 300 K (room temperature). Note the differences when comparing to Figure 13 in Section 5.6; the large temperature delta affected the accuracy of the calibration.

Many repeated measurements have shown that for a given system setup, the effect of a temperature delta on a calibration is very repeatable in terms of using a calibration taken at temperature A and applying it to a measurement at temperature B. The case below in Figure 18 shows an approximate worst case scenario in terms of affecting the calibration due to the very large (~290 K) temperature change. For smaller temperature changes, the effect on performance is much smaller; with temperature deltas of 10–20 K the affect is negligible. Nonetheless, for the most accurate measurements at a given temperature, it is recommended that the calibration be performed with the system operating at that temperature.

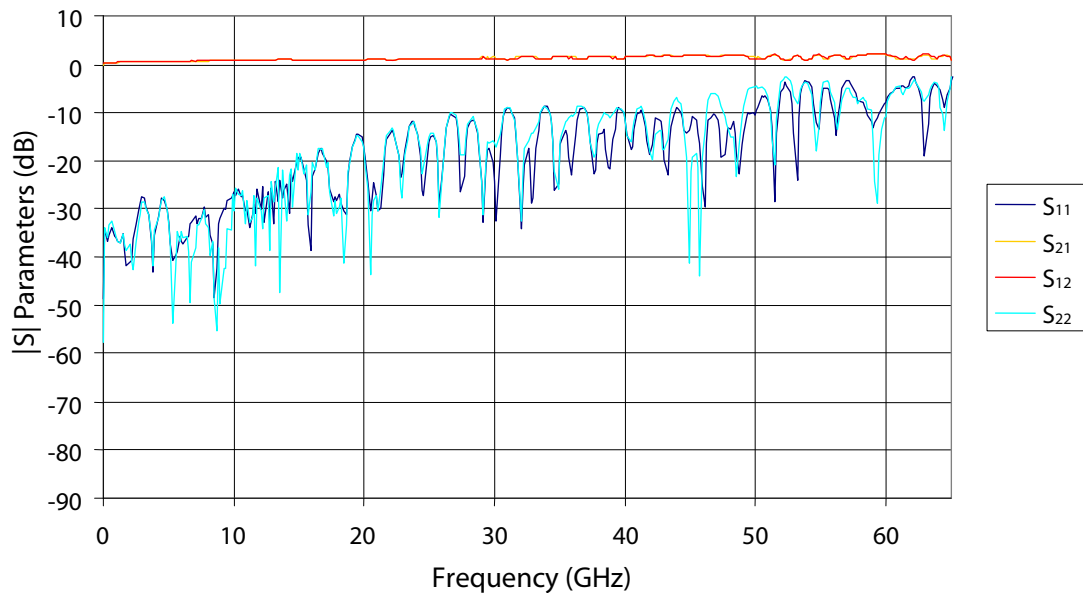


FIGURE 18: Microwave probes measured at 4.2 K after calibration with CS-5 substrate performed at 300 K

5.9 Time Domain Reflectometry (TDR) Measurements

The time domain reflectometry (TDR) option of the Anritsu VNA allows us to view the S_{11} reflection coefficient in the time domain to gain some information about the probe station signal path by showing us (in relative time) the places in the system that are points of reflection. Knowing the speed of light and the velocity factor of the transmission lines used in the setup, we can translate the time plot to physical distances. Reflections will occur at discontinuities in impedance. In a microwave setup that involves coaxial threaded connectors — reflections will occur at connector mating points. An unusually large reflection at a connector mating point can signify a bad or poor connection; however, even if the connectors are kept clean and torqued to the proper amount, a reflection is inevitable (i.e., the price you pay for the flexibility of being able to connect/disconnect). In our system, an additional point for an impedance discontinuity is the transition from probe tips down to the DUT substrate. Therefore, what we want to do here is identify the point in time that corresponds to the probe tips touching down on the substrate, and to evaluate the reflection coming from that point relative to the other reflections from the mating connectors.

Figure 19 corresponds to the TDR transform of the S_{11} data shown in Figure 10 of a pair of 67 GHz probes on a through test point of the CS-5 substrate. The peaks in the S_{11} TDR trace represent reflection points in the signal path that can be related to the round-trip path of the time that it takes the signal to be sent to, reflect, and return to the test measurement reference plane. Recall that for the measurements shown in Figure 10, we used the calibration in section 5.1 that placed the VNA measurement reference plane at the 1.85 mm input connectors of the probe arms. We want to place the reference there because these measurements allow us to evaluate the probe station system response. With this calibration, time 0 on the plots below corresponds to the 1.85 mm input connector that is connected to port 1. Therefore, the reflection shown at time 0 corresponds to the first connector mating between the VNA test cable and the probe arm.

Since multiple reflections from various impedance mismatches often complicate a TDR trace, it is sometimes difficult to correlate other reflection points. The trace data shown in Figure 20, however, can help us do this. By raising the probe tips for the probe on port 1 off of the CS-5 substrate, we can get a point of reference, since we know that with the probe tips up in the air (i.e., open circuit), there will be a large reflection at the probe tips. In Figure 20, we see the large reflection at about 1.2 ns. Having this reference point bounds our analysis of the reflections seen by port 1 to the time period from 0 to 1.2 ns. We can have pretty good certainty that in this time period we are seeing first-order reflections (since multiple reflections will have longer paths to traverse). The several peaks after 1.2 ns are due to multiple reflections.

We can now look back at Figure 19 to determine the physical points of the reflections up to 1.2 ns. The reflection at 1.0 ns is due to the connector that connects the semi-rigid cable in the probe arm to the probe itself. In looking at the reflection at 1.2 ns (corresponding to the probe tips touching the substrate), we see that it is on the order of 10–12 dB below the reflections from the connector reflections at 0 and 1 ns. This tells us that the probe tips are well seated on the test substrate and that the GSG microwave probes effectively launch the microwave energy from the probe down to the pads on the test substrate with minimal reflected energy.

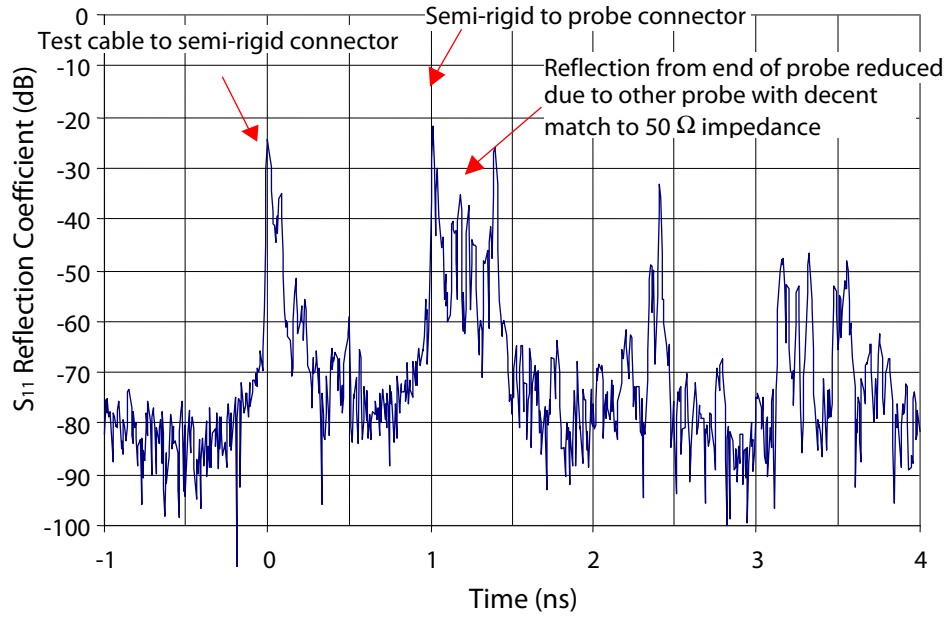


FIGURE 19: TDR measurement with both port 1 and port 2 probe tips seated on a through test point

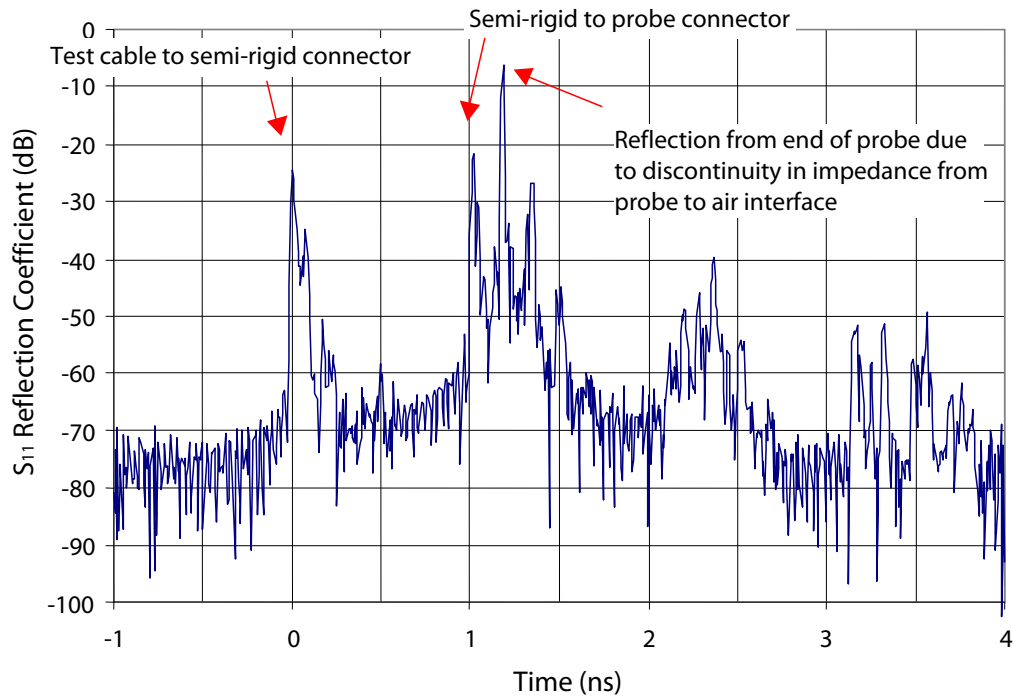


FIGURE 20: TDR measurement with port 1 probe tip lifted off of the substrate; note the large reflection at ~1.2 ns, which corresponds to the end of the probe tip

5.10 Measurements with a Broken Probe Tip

Figure 21 below shows the response for a pair of 200 μm pitch 67 GHz probes from 40 MHz to 65 GHz placed on a 50 Ω through test structure on the CS-5 calibration substrate. These measurements were made exactly the same as in Section 5.3 and Figure 10, except that the probe on port 1 had a broken ground tip. These results are presented here to show how important the structure of the probe tips are, and that damage to any of the three GSG pins on either probe will significantly degrade performance. The transmission coefficients S_{21}/S_{12} for this case drop down to -50 dB, which are unusable. Note that for the broken probe on port 1, the reflection coefficient S_{11} is above -10 dB for almost the entire frequency band signifying that most of the signal sent by that port is being reflected right back to that port and not getting to the DUT.

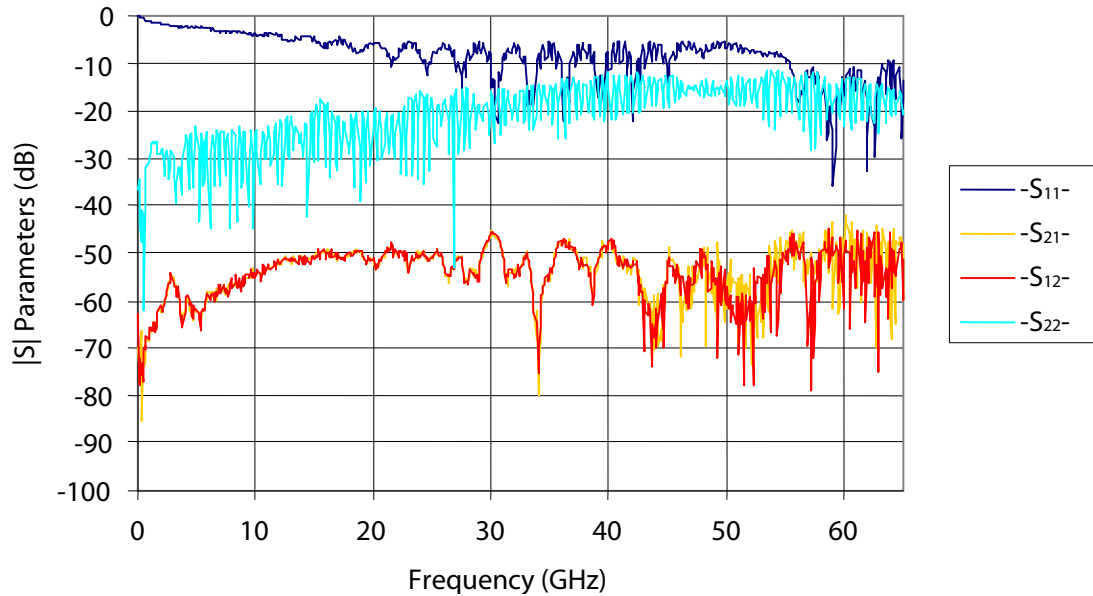


FIGURE 21: 67 GHz probes with probe on port 1 having a broken ground tip

APPENDIX A — S (Scattering) Parameters

A scattering matrix (S-parameter matrix) is one way to describe the operation of a linear, time-invariant two-port circuit. A 2-port network is defined as any linear device where a signal goes in one side and comes out the other. The S-parameter matrix is rapidly becoming very popular as a way to characterize connectors and cables for high-speed applications. The measurement setup associated with S parameters is as follows.

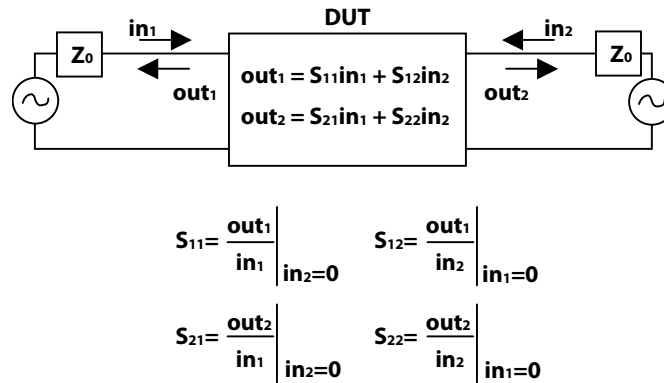


FIGURE 1: A 2-port S-parameter matrix records the reflection coefficients and transmission gain from both sides of the DUT.

From the test equipment, two cables having characteristic impedance Z_0 lead to the left and right sides, respectively, of the device under test (DUT).

Using the first (left-side) cable, a sinusoidal signal (in_1) of unit amplitude is injected into the DUT. The test equipment records the amplitude and phase of the signal (out_1) reflected back onto the first cable from the DUT, and also the amplitude and phase of the signal (out_2) conveyed through the DUT to the second cable on the other side.

Using the second (right-side) cable, another sinusoidal signal (in_2) of unit amplitude is injected into the DUT. The test equipment records the amplitude and phase of the signal (out_2) reflected from the right side of the DUT, and the amplitude and phase of the signal (out_1) conveyed through the DUT to the other (left) side. The complete S-parameter matrix is a combination of these four basic measurements.

The four elements of an S-parameter matrix may be reported as complex numbers (with real and imaginary parts) or in logarithmic units (as dB magnitude and phase).

[Note that the procedure above provides a model for the calculation of circuit performance only at one single frequency. The entire procedure is usually performed on a dense grid of frequencies spanning the range of interest, such that the parameters S_{11} , etc., are all functions of frequency.]

Provided that the reflection coefficients S_{11} and S_{22} are relatively small, you may estimate the effect of cascading several 2-port networks by merely multiplying the S_{21} coefficients of the individual components (or, if they are in logarithmic units, by adding the dB values of the S_{21} coefficients). Such a calculation determines, **to first order**, the magnitude and phase of a signal that propagates straight through the cascade proceeding from left to right through each component. This is the beauty of S-parameter analysis, and one key reason it is used in the design of highly cascaded systems like radio receivers and chains of linear amplifiers.

Unfortunately, the overall transfer function of a highly cascaded system equals the product of the S_{21} terms **only** when the reflections are negligible. If the reflections are significant, the gain does NOT equal the product of S_{21} terms.